



HAL
open science

Investigation of two-photon polymerized microstructures using fluorescence lifetime measurements

Xingyu Wu, Mehdi Belqat, Benjamin Leuschel, Guillaume Noirbent, Frédéric Dumur, Karine Mougin, Arnaud Spangenberg

► To cite this version:

Xingyu Wu, Mehdi Belqat, Benjamin Leuschel, Guillaume Noirbent, Frédéric Dumur, et al.. Investigation of two-photon polymerized microstructures using fluorescence lifetime measurements. *Polymer Chemistry*, 2022, 13 (20), pp.2902-2906. 10.1039/d1py01728d . hal-04274282

HAL Id: hal-04274282

<https://cnrs.hal.science/hal-04274282>

Submitted on 7 Nov 2023

HAL is a multi-disciplinary open access archive for the deposit and dissemination of scientific research documents, whether they are published or not. The documents may come from teaching and research institutions in France or abroad, or from public or private research centers.

L'archive ouverte pluridisciplinaire **HAL**, est destinée au dépôt et à la diffusion de documents scientifiques de niveau recherche, publiés ou non, émanant des établissements d'enseignement et de recherche français ou étrangers, des laboratoires publics ou privés.

COMMUNICATION

Investigation of two-photon polymerized microstructures using fluorescence lifetime measurements

Received 00th January 20xx,
Accepted 00th January 20xx

Xingyu Wu, ^{†a} Mehdi Belqat, ^{†a} Benjamin Leuschel, ^a Guillaume Noirbent, ^b Frédéric Dumur, ^b Karine Mougín ^a and Arnaud Spangenberg*^a

DOI: 10.1039/x0xx00000x

We report the use of fluorescence lifetime measurements for investigating two-photon polymerization. For this purpose, a molecular rotor was successfully exploited as viscosity probe to reveal heterogeneity in multi-material microstructures made by two-photon polymerization. Furthermore, a correlation between laser intensity and local viscosity changes in the polymerized microstructures was established.

In recent years, two-photon stereolithography (TPS), based on the non-linear absorption of light, has emerged as a powerful additive manufacturing technology to create arbitrary and complex 3D or 4D microstructures, made of single or multi-materials.¹⁻⁵ By tightly focusing an ultrafast laser beam into a photoresist, photopolymerization can be induced within the focal volume and consequently create structures whose resolution can reach below the diffraction limit.⁶⁻⁹ Owing to the increasing importance of TPS for rapid prototyping of 3D structures at the microscale, numerous studies have been performed to characterize the resulting microstructures and several methods have been implemented to elucidate the mechanisms underlying the two-photon polymerization (TPP) reaction.^{10,11}

Surprisingly, although the resin viscosity is known to play a crucial role in photopolymerization,¹² this parameter has been scarcely studied in the context of TPP. For instance, Zandrini *et al.* have very recently investigated the impact of resin viscosity on the linewidth, polymerization and damage thresholds, dynamic range and fabrication resolution.¹³ Sakellari *et al.* have developed a method for high-resolved TPS based on quencher diffusion which allows to produce microstructures with resolution comparable to those obtained via STED-like lithography.¹⁴ While these examples highlight the importance to take into consideration the influence of viscosity on the final properties of fabricated microstructures and its impact on the

kinetics of TPP, the changes in viscosity occurring before and after polymerization were not investigated. Although several methods, such as rheometry, viscometry and dilatometry have been commonly employed to measure viscosities,^{15,16} these approaches probe only on a macroscopic scale and are not adapted to investigate samples as small as those produced in TPP. Meanwhile, fluorescence-based techniques have attracted extensive attention, owing to their high sensitivity, large contrast and high resolution.^{17,18} Molecular rotors as fluorophores have been highlighted as promising candidates for measurements of local viscosity.¹⁹⁻²² In this class of fluorophores, the non-radiative decay of the excited state is strongly influenced by the viscosity of the medium. When the viscosity increases, the intramolecular rotation becomes slower and the non-radiative decay consequently decreases. Thus, both the fluorescence quantum yield and the lifetime of molecular rotors can be correlated with the viscosity of the surrounding environment.²³ Measurements based on fluorescence quantum yields suffer from difficulties in distinguishing between viscosity and other factors which may affect the fluorescence intensity, such as fluctuations of the fluorophore's concentration or variations in the optical properties of the medium.²⁴ To solve this problem, a ratiometric approach has been developed using probes which incorporate two independent fluorophores – one is a molecular rotor, another one is unaffected by viscosity – into one compound.^{25,26} However, this approach requires additional synthesis and calibration steps, rendering this method much more complex. Compared with fluorescence intensity-based measurement, fluorescence lifetime detection offers a major advance due to easy system calibration, ultrasensitive detection and the possibility to be coupled with a spatially resolved imaging (e.g. FLIM, Fluorescence Lifetime Imaging Microscopy), which is a powerful technique to distinguish the unique molecular environment of fluorophores.²⁷

In our present work, we used fluorescence lifetime measurements to investigate two-photon polymerization. We first demonstrated how local viscosity can be used to probe heterogeneity in multi-material microstructures made by two-photon polymerization. Then, we investigated the impact of writing conditions on local viscosity of undeveloped

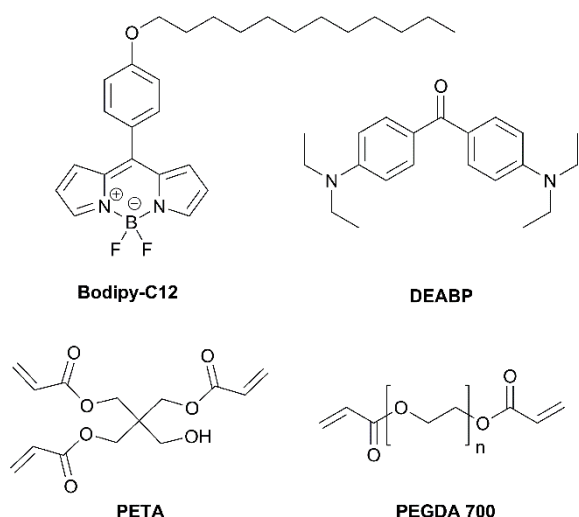
^a Institut de Science des Matériaux de Mulhouse (IS2M), CNRS – UMR 7361, Université de Haute Alsace, 15 rue Jean Starcky, 68057 Mulhouse, France
Université de Strasbourg, France

*E-mail: arnaud.spangenberg@uha.fr

^b Aix Marseille Univ, CNRS, ICR, UMR 7273, F-13397 Marseille – France

[†] These authors contributed equally to this paper.

Electronic Supplementary Information (ESI) available. See DOI: 10.1039/x0xx00000x



Scheme 1. Chemical structures of the molecular rotor (Bodipy-C12), the photoinitiator (DEABP) and the monomers (PETA, PEGDA 700) used in this work.

polymerized microstructures. For these purposes, a molecular rotor, Bodipy-C12 (Scheme 1 and Figure S1-3 for synthesis and characterization) was chosen because 1) its lifetime sensitivity covers a wide viscosity range; 2) the lifetime, at least at high viscosities, is only weakly affected by the polarity and temperature of the environment; and 3) mono exponential decays of the excited state allows for straightforward data interpretation.^{19,27-31} After introducing this probe and a photoinitiator (4,4'-bis(N,N-diethylamino) benzophenone, DEABP) into two different multi-functional monomer and oligomer, namely pentaerythritol triacrylate (PETA) and poly(ethylene glycol) diacrylate 700 (PEGDA 700) respectively (Scheme 1), we measured the fluorescence lifetimes before and after two-photon polymerization.

To exclude any influence of the probe itself on the photopolymerization process, FTIR experiments were conducted on the two acrylate resins under UV irradiation in presence and absence of Bodipy-C12. From Figure S4a and S4b, showing the evolution of double bond (C=C) conversion, it is obvious that without photoinitiator, but with Bodipy-C12 (10^{-4} mol L⁻¹) in the formulation, the conversion of C=C in both PETA and PEGDA 700 remains close to 0. Adding Bodipy-C12 (10^{-4} mol L⁻¹) to resin formulations PETA/DEABP (1 wt% in PETA) and PEGDA/DEABP (1 wt% in PEGDA 700) does not influence the respective photopolymerization as well, compared with the same formulation without Bodipy-C12. Thanks to these results, we can conclude that Bodipy-C12 does not play a positive or negative role in the photopolymerization reaction.

In order to establish the calibration plot of fluorescence lifetime τ versus viscosity η for Bodipy-C12, we performed fluorescence lifetime measurements of Bodipy-C12 in glycerol-methanol mixtures (Figure S5a), whose viscosity can be altered in a wide range (0.5–950 cP). The plot of $\log_{10}\tau$ versus $\log_{10}\eta$ (Figure S5b) shows a linear fit. From these data, we can see the fluorescence lifetime of Bodipy-C12 increases from 0.78 ns to 3.44 ns with increasing solution viscosity from 28 to 950 cP. The fluorescence lifetime follows the Forster–Hoffmann equation (see ESI,

equations 1 and 2) in this viscosity range, since a good linear correlation with a slope of 0.4 is observed.^{27,32,33}

After calibration, the fluorescence lifetime of Bodipy-C12 in PETA and PEGDA 700 was determined before and after polymerization. The microstructures were fabricated with an exposure time of 10 ms and the laser intensity was set to 9.40 mW cm⁻² and 17.8 mW cm⁻² respectively. Then, the microstructures were developed in ethanol to remove the unpolymerized resin. Before two-photon polymerization, the fluorescence lifetime in PETA and PEGDA-700 based resins are 1.5 ns and 1.03 ns, respectively. In contrast, after polymerization, the fluorescence lifetime in both microstructures increases, in PETA to 4.09 ns and in PEGDA-700 to 2.9 ns. Table 1 lists all fluorescence lifetime values. The fluorescence decay curves for both before and after polymerization on a logarithmic scale are presented in Figure 1, which evidently shows that after two-photon polymerization, the fluorescence lifetime increases. This can be explained by the local increases in viscosity after photopolymerization. Here, it is worth noting that the curves obtained from the resins before photopolymerization were fitted using a mono-exponential function ($n=1$), while after polymerization, a bi-exponential function ($n=2$) was used to appropriately fit the measured time-correlated single photon counting (TCSPC) curves. The weighted average fluorescence lifetime (as defined in ESI equations 3 and 4) was used to represent the fluorescence lifetime in the microstructures. For both cases, the long lifetime is predominant. The short lifetime may be ascribed to the presence of residual monomers and short polymer chains trapped inside the polymerized microstructures even after development. This indicates that a certain heterogeneity exists in these microstructures at the molecular level. Furthermore, to illustrate the potential of our approach, a 100 μm x 60 μm rectangular microstructure formed by 20 μm x 20 μm squares made from PETA and PEGDA based resins was fabricated by TPS (Figure 2a). Whereas it would be complicated to discriminate between the parts made from PEGDA and those made from PETA by using only scanning electron microscopy (SEM), the distinct fluorescence lifetime of Bodipy-C12 observed for each polymer allows to clearly visualise the different parts using FLIM

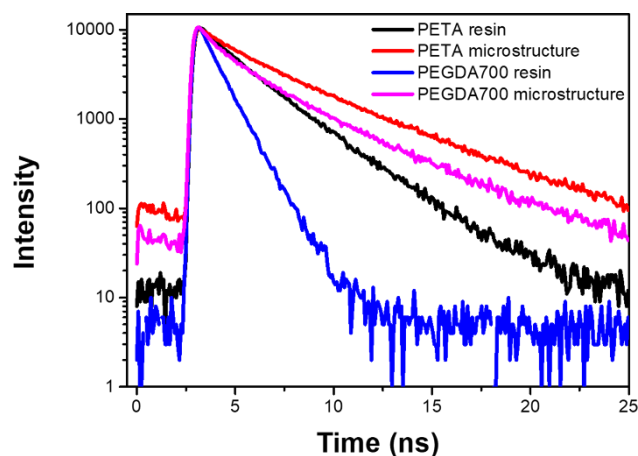


Figure 1. Fluorescence decay curves of Bodipy-C12 in PETA (black) and PEGDA-700 (blue) resin before polymerization and in two-photon fabricated microstructures based on PETA (red) and PEGDA-700 (pink) respectively.

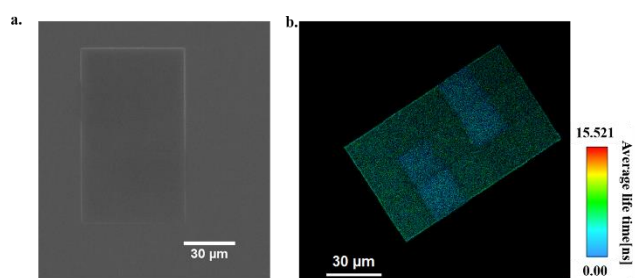


Figure 2. SEM images (a) and lifetime images (b) of a pattern made by PETA (green) and PEGDA 700 (blue).

as depicted in Figure 2b. The simplicity of FLIM to detect different materials or to reveal micro-heterogeneity opens new perspectives for the characterization of multi-material printed objects.

Next, the fluorescence lifetime of Bodipy-C12 in PETA and PEGDA 700 microstructures made at different intensities was studied. Here, in order to measure the fluorescence lifetime of Bodipy-C12 in microstructures at low laser intensities, the development by ethanol was omitted, thus limiting the risk of losing the most fragile structures. In case of PETA microstructures, according to the fluorescence decays and FLIM images (Figure S6), no significant change of the fluorescence lifetime is noticed with respect to the laser intensity ranging from 6.08 mW cm⁻² to 16.72 mW cm⁻² (Table S1). Conversely, the lifetime gradually increases with increasing intensity used for the fabrication of PEGDA 700 microstructures (Figure 3). In FLIM images, the color of the microstructure made at 7.72 mW cm⁻² is blue, while the microstructure made at 19.70 mW cm⁻² appears green, which indicates a longer lifetime. To better understand the evolution of the lifetime of Bodipy-C12 in microstructures made at different intensities, the lifetime components ($n=2$ as mentioned above) were analyzed. As shown in Figure 4, the change of the weighted average fluorescence lifetime is not only caused by the change of the two lifetimes (long lifetime and short lifetime, Figure 4a) but also by a significant change in their respective amplitudes

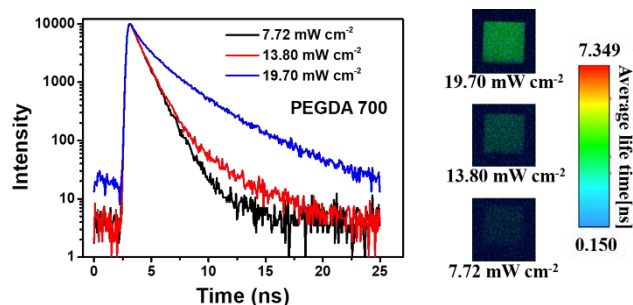


Figure 3. Fluorescence decay curves and fluorescence lifetime images of Bodipy-C12 in two-photon fabricated microstructures made from PEGDA 700 at different intensities.

(Figure 4b). In microstructures made from 7.72 mW cm⁻² to 8.56 mW cm⁻², both fluorescence lifetimes and their amplitudes keep stable. The long lifetime is around 2 ns and the short lifetime is around 1 ns and their amplitude fractions are 10% and 90%, respectively. When the intensity increases from 8.56 mW cm⁻² to 13.80 mW cm⁻², the long lifetime gradually increases from 2 ns to 3 ns and then to 3.6 ns with slightly increasing amplitude fractions, whereas the short lifetime remains constant. The slight increase of the amplitude fraction causes only a small increase of the weighted average fluorescence lifetime, even though the long lifetime changes significantly. From 13.80 mW cm⁻² to 19.7 mW cm⁻², the long lifetime remains constant and the short lifetime has a slight change from 1 ns to 1.3 ns. However, the amplitude fraction of long lifetime significantly increases from 15 % at 13.80 mW cm⁻² to 70 % at 16.0 mW cm⁻², which explains the prominent increase of the weighted average fluorescence lifetime from 1.1 ns to 2.3 ns. This is why we can see a large gap between 13.80 mW cm⁻² and 16.0 mW cm⁻² in the fluorescence decay curve of Bodipy-C12 in PEGDA 700 microstructures in Figure 3. The appearance of two different lifetimes points to the presence of Bodipy-C12 in distinguishable local environments. The long lifetime shows the significant changes that occur when increasing intensity for the fabrication of microstructures.

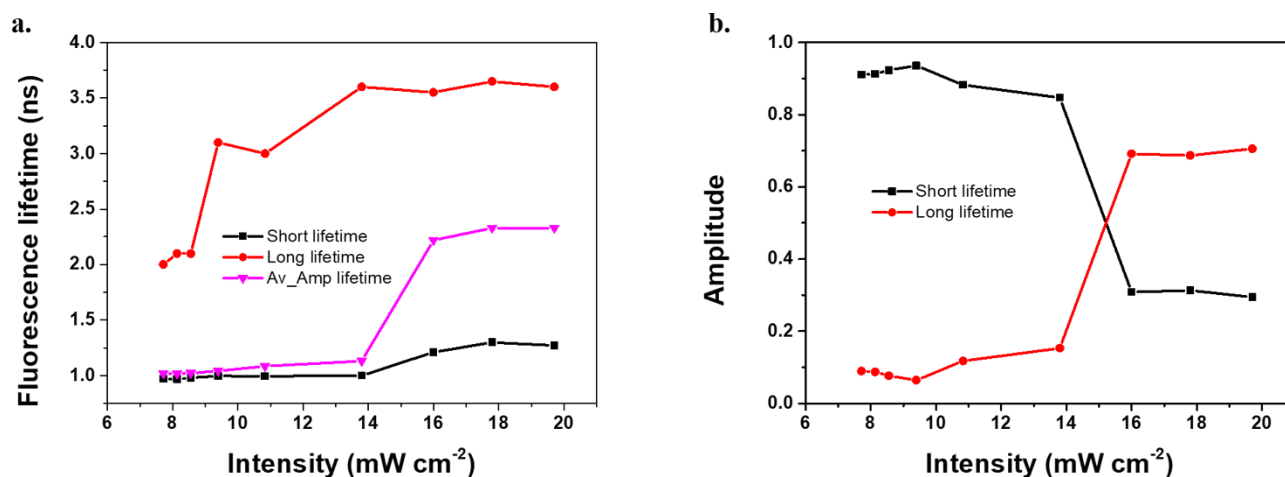


Figure 4. Fluorescence lifetimes (a) and amplitudes (b) of the Bodipy-C12 with respect to the laser intensity used for PEGDA 700 two-photon polymerization. From these data and the corresponding amplitudes, the weighted average fluorescence lifetime (pink triangles) was calculated (see the equation in the ESI).

COMMUNICATION

Table 1. Summary of Fluorescence lifetimes and amplitudes.

	Long lifetime (ns)	Amplitude of long lifetime	Short lifetime (ns)	Amplitude of short lifetime	Weighted average fluorescence lifetime (ns)	χ^2 ^a
Resins						
PETA resin			1.5 ± 0.27			0.916
PEGDA 700 resin			1.03 ± 0.0055			0.961
Developed microstructures						
PETA 9.40 mW cm ⁻²	5 ± 0.12	0.87	1.9 ± 0.17	0.13	4.09 ± 0.023	0.986
PEGDA 700 17.8 mW cm ⁻²	4.11 ± 0.079	0.80	1.32 ± 0.074	0.20	2.9 ± 0.02	0.953
Undeveloped microstructures						
PEGDA 700 7.72 mW cm ⁻²	2 ± 0.22	0.09	0.97 ± 0.0098	0.91	1.02 ± 0.0061	1.121
PEGDA 700 8.14 mW cm ⁻²	2.1 ± 0.2	0.09	0.97 ± 0.016	0.91	1.02 ± 0.0056	0.935
PEGDA 700 8.56 mW cm ⁻²	2.1 ± 0.44	0.08	0.98 ± 0.031	0.92	1.02 ± 0.0091	1.065
PEGDA 700 9.40 mW cm ⁻²	3.1 ± 0.32	0.06	1 ± 0.0077	0.94	1.04 ± 0.0059	1.040
PEGDA 700 10.83 mW cm ⁻²	3 ± 0.25	0.12	1 ± 0.012	0.88	1.08 ± 0.0064	1.051
PEGDA 700 13.80 mW cm ⁻²	3.6 ± 0.15	0.15	1 ± 0.01	0.85	1.13 ± 0.0089	0.857
PEGDA 700 16.0 mW cm ⁻²	3.55 ± 0.083	0.69	1.21 ± 0.049	0.31	2.22 ± 0.024	1.203
PEGDA 700 17.8 mW cm ⁻²	3.65 ± 0.076	0.69	1.3 ± 0.045	0.31	2.33 ± 0.019	1.187
PEGDA 700 19.7 mW cm ⁻²	3.6 ± 0.05	0.71	1.27 ± 0.046	0.29	2.33 ± 0.012	1.128

a. χ^2 as a goodness of fit parameter. $\chi^2 \approx 1$ indicates a good fit.

We assume that the probe is in regions where the crosslinking of the polymer evolves gradually and thus hinders the rotation of the molecular rotor. The highly cross-linked regions grow larger in the microstructures made at higher intensities and therefore the fraction of the probe with a longer lifetime is enhanced. In contrast, the short lifetime is not as strongly influenced by the intensity used for the microstructure fabrications. The probe should be in the less cross-linked regions, where the rotation of molecular rotor is less confined. These results show that local viscosity determined by FLIM can be an effective method for studying the impact of fabrication processing on the final properties of microstructures.

Conclusions

We have demonstrated that fluorescence lifetime measurement is an effective method for characterizing microstructures fabricated by two-photon polymerization. The dependency of fluorescence lifetime of Bodipy-C12 with respect to its local environment was exploited to reveal heterogeneity in multi-material microstructures based on PETA and PEGDA-700. Furthermore, a correlation between writing conditions and local viscosity changes within polymerized microstructures made from PEGDA-700 was established by investigating the fluorescence lifetime changes of the molecular rotor. Based on these results, we anticipate that fluorescence lifetime measurement can be successfully applied to explore kinetics of

two-photon polymerization or probe the 4D character of active 3D structures made by TPP.

Acknowledgements

The Agence Nationale de la Recherche (ANR agency) is acknowledged for its financial support through the PhD grants of Guillaume Noirbent (ANR-17-CE08-0054 VISICAT project) and Mehdi Belqat (ANR-16-CE08-347 0020 2PhotonInsight project). The authors also thank the ANR agency, the Institut Carnot MICA, the M2A and the Region Grand Est (Institutional Research Grant: MIPPI4D) for financial support allowing the purchase of FLIM equipment.

Conflicts of interest

There are no conflicts to declare.

Notes and references

- H.-B. Sun, T. Tanaka, K. Takada and S. Kawata, *Appl. Phys. Lett.*, 2001, **79**, 1411-1413.
- A. Ovsianikov, J. Viertl, B. Chichkov, M. Oubaha, B. MacCraith, I. Sakellari, A. Giakoumaki, D. Gray, M. Vamvakaki, M. Farsari and C. Fotakis, *ACS Nano*, 2008, **2**, 2257-2262.
- C. Barner-Kowollik, M. Bastmeyer, E. Blasco, G. Delaittre, P. Müller, B. Richter and M. Wegener, *Angew. Chem., Int. Ed.*, 2017, **56**, 15828-15845.

4. M. Hippler, E. Blasco, J. Qu, M. Tanaka, C. Barner-Kowollik, M. Wegener and M. Bastmeyer, *Nat. Commun.*, 2019, **10**, 232.
5. C. A. Spiegel, M. Hippler, A. Münchinger, M. Bastmeyer, C. Barner-Kowollik, M. Wegener and E. Blasco, *Adv. Funct. Mater.*, 2020, **30**, 1907615.
6. M. Deubel, G. von Freymann, M. Wegener, S. Pereira, K. Busch and C. M. Soukoulis, *Nat Mater*, 2004, **3**, 444-447.
7. W. Haske, V. W. Chen, J. M. Hales, W. Dong, S. Barlow, S. R. Marder and J. W. Perry, *Opt. Express*, 2007, **15**, 3426-3436.
8. S. Kawata, H.-B. Sun, T. Tanaka and K. Takada, *Nature*, 2001, **412**, 697-698.
9. V. Hahn, P. Kiefer, T. Frenzel, J. Qu, E. Blasco, C. Barner-Kowollik and M. Wegener, *Adv. Funct. Mater.*, 2020, **30**, 1907795.
10. C. N. LaFratta and T. Baldacchini, *Micromachines*, 2017, **8**, 101.
11. E. Skliutas, M. Lebedevaite, E. Kabouraki, T. Baldacchini, J. Ostrauskaite, M. Vamvakaki, M. Farsari, S. Juodkakis and M. Malinauskas, *Nanophotonics*, 2021, **10**, 1211-1242.
12. E. Andrzejewska and A. Marcinkowska, *J. Appl. Polym. Sci.*, 2008, **10**, 2780-2786.
13. T. Zandrini, N. Liaros, L. J. Jiang, Y. F. Lu, J. T. Fourkas, R. Osellame and T. Baldacchini, *Opt. Mater. Express*, 2019, **9**, 2601-2616.
14. I. Sakellari, E. Kabouraki, D. Gray, V. Purlys, C. Fotakis, A. Pikulin, N. Bityurin, M. Vamvakaki and M. Farsari, *ACS Nano*, 2012, **6**, 2302-2311.
15. C. W. Macosko, *Rheology: Principles, Measurements, and Applications*, Wiley-VCH, Minneapolis, 1994.
16. O. Okay, D. Kaya and O. Pekcan, *Polymer*, 1999, **40**, 6179-6187.
17. M. Beija, M.-T. Charreyre and J. M. G. Martinho, *Prog. Polym. Sci.*, 2011, **36**, 568-602.
18. A. M. Breul, M. D. Hager and U. S. Schubert, *Chem. Soc. Rev.*, 2013, **42**, 5366-5407.
19. J. M. Nölle, C. Jüngst, A. Zumbusch and D. Wöll, *Polym. Chem.*, 2014, **5**, 2700-2703.
20. F. Jbilou, I. N. Georgousopoulou, S. Marinkovic, S. Vouyiouka, C. D. Pappaspyrides, B. Estrine, P. Dole, A. Cottaz and C. Joly, *Eur. Polym. J.*, 2016, **78**, 61-71.
21. M. R. Bittermann, M. Grzelka, S. Woutersen, A. M. Brouwer, and D. Bonn, *The Journal of Physical Chemistry Letters*, 2021, **12**, 3182-3186.
22. A. Polita, S. Toliautas, R. Zvirblis and A. Vysniauskas, *Phys. Chem. Chem. Phys.*, 2020, **22**, 8296.
23. M. A. Haidekker and E. A. Theodorakis, *Org. Biomol. Chem.*, 2007, **5**, 1669-1678.
24. Y. Wu, M. Štefl, A. Olzyńska, M. Hof, G. Yahioglu, P. Yip, D. R. Casey, O. Ces, J. Humpolíčková and M. K. Kuimova, *Phys. Chem. Chem. Phys.*, 2013, **15**, 14986-14993.
25. M. A. Haidekker, T. P. Brady, D. Lichlyter and E. A. Theodorakis, *J. Am. Chem. Soc.*, 2006, **128**, 398-399.
26. M. K. Kuimova, S. W. Botchway, A. W. Parker, M. Balaz, H. A. Collins, H. L. Anderson, K. Suhling and P. R. Ogilby, *Nature Chemistry*, 2009, **1**, 69-73.
27. M. K. Kuimova, G. Yahioglu, J. A. Levitt and K. Suhling, *J. Am. Chem. Soc.*, 2008, **130**, 6672-6673.
28. A. Vysniauskas, M. Qurashi, N. Gallop, M. Balaz, H. L. Anderson and M. K. Kuimova, *Chem. Sci.*, 2015, **6**, 5773-5778.
29. M. R. Dent, I. López-Duarte, C. J. Dickson, N. D. Geoghegan, J. M. Cooper, I. R. Gould, R. Krams, J. A. Bull, N. J. Brooks and M. K. Kuimova, *Phys. Chem. Chem. Phys.*, 2015, **17**, 18393-18402.
30. T. T. Vu, R. Meallet-Renault, G. Clavier, B. A. Trofimov and M. K. Kuimova, *J. Mater. Chem. C*, 2016, **4**, 2828-2833.
31. A. Vysniauskas, I. Lopez-Duarte, N. Duchemin, T. T. Vu, Y. L. Wu, E. M. Budynina, Y. A. Volkova, E. P. Cabrera, D. E. Ramirez-Ornelas and M. K. Kuimova, *Phys. Chem. Chem. Phys.*, 2017, **19**, 25252-25259.
32. T. Förster and G. Hoffmann, *Z. Phys. Chem.*, 1971, **75**, 63-76.
33. J. A. Levitt, M. K. Kuimova, G. Yahioglu, P.-H. Chung, K. Suhling and D. Phillips, *J. Phys. Chem. C*, 2009, **113**, 11634-11642.